# BEYOND OMNIDIRECTIONALITY: INVESTIGATING THE DESIGN AND USE OF CIRCULAR ANTENNA ARRAYS

Augustine Law[1], Lee Yann Ze Darryl[1], Ang Teng Wah[2], Huang Ying Ying[2], Lim Zi Wei[2]
[1]Raffles Institution (Secondary), 1 Raffles Institution Ln, Singapore 575954
[2]DSO National Laboratories, 12 Science Park Drive Singapore 118225

## ABSTRACT

Smart antennas can toggle between directional and omnidirectional radiation through electronic manipulation and without physical change, which offers an adaptable alternative to conventional monopole antennas. This project proposes a circular array consisting of 8 monopole elements and a centre reflector, designed to operate in the 7-9GHz band and fabricated using 50Ω SMA connectors. A monopole height of 9mm, a small array radius of 20mm and a reflector height of 17mm are optimal for omnidirectional and directional coverage, providing even coverage, high gain and low S11 performance. The array was fabricated with metallized 3D-printed plastic andtested with a VNA to verify the simulated results. Our measured results show correspondence with the simulated result, displaying below -8dB return loss bandwidth from 6-12GHz. To maximize the directional gain of the array, phase changes were applied to some elements, allowing us to steer the radiation in any desired direction. A general formula for beamsteering was derived, allowing highly directed coverage in any desired direction. Through toggling between a 3-port and 8-port excitation mode, the array achieves an average realized omnidirectional gain of -0.68dB and a directional gain range of 6.8-7.2dB. Overall, the fabricated array provides more versatile radio coverage over conventional monopole antennas.

## INTRODUCTION

Conventional monopole antennas are omnidirectional in nature, which causes it to suffer in long-distance radio transmission. In recent years, smart antennas have gained attention due to their adaptive features. An intelligent antenna has an array of individual radiation elements which are placed in a particular configuration (linear, circular or matrix). Instead of employing mechanical changes in the structure, but by changing the characteristics of the applied signals, the array can present different gains according to the desired direction of propagation [1]. This manipulation involves changes in phase excitation of the antenna elements [2]. We hypothesise that our proposed circular array is able to address the lack of far-range coverage by monopoles.

## METHODS AND RESULTS

Parametric sweeps were conducted using Ansys HFSS. S11 graphs were plotted to observe the return loss characteristics and gain plots were used to study the simulated radiation pattern. To simulate the circular array, 8 monopoles with radius 0.635mm were used in accordance with SMA connector dimensions for convenient fabrication, which allows for the elements to be close to each other without overlapping. A cylindrical reflector in the centre of the array directs radiation outwards and improves S11 performance. The distance between any one element and the reflector is kept at 9mm, following the quarter wavelength principle. We analysed the effect of the array radius and reflector height on the performance of the array in both its directional and omnidirectional modes. Finally, we investigated the effect of changing the phases of the excitations on the gain of the array.

After simulation, the array is fabricated with 3D-printed Polylactic Acid, metallised with copper and aluminium tape for the ground and reflector respectively. 8 SMA connectors of height 9mm were adhered to the ground. The active S11 performance of the array was tested and verified using a Vector Network Analyser (VNA).

1. Single monopole antenna

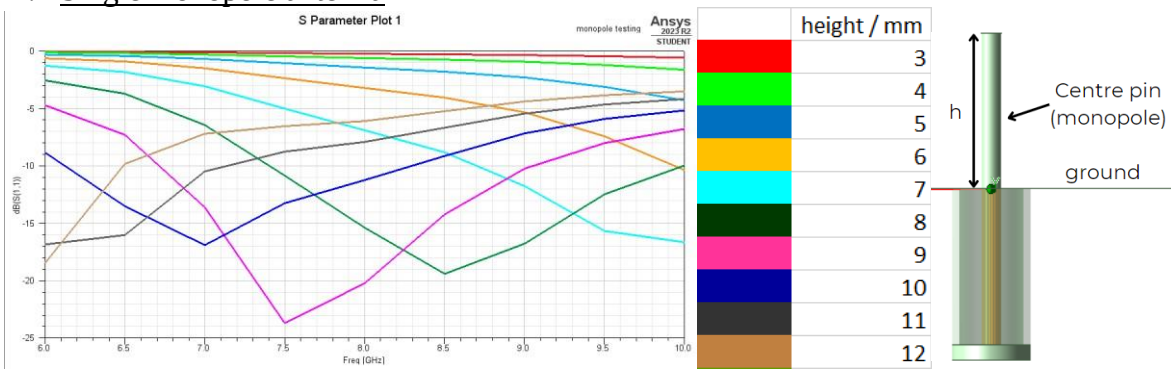


**Fig. 1**: (a) S Parameter for monopole antenna of height 3-12mm (b) Model of SMA connector

The monopole antenna displays a 10dB return loss from 6.7-9GHz (2.3GHz bandwidth) at height 9mm, which suits our proposed working range of 7-9GHz. This height is approximately a quarter of the wavelength at 8GHz, that is 37.5mm.

2. Circular array (Omnidirectional mode)

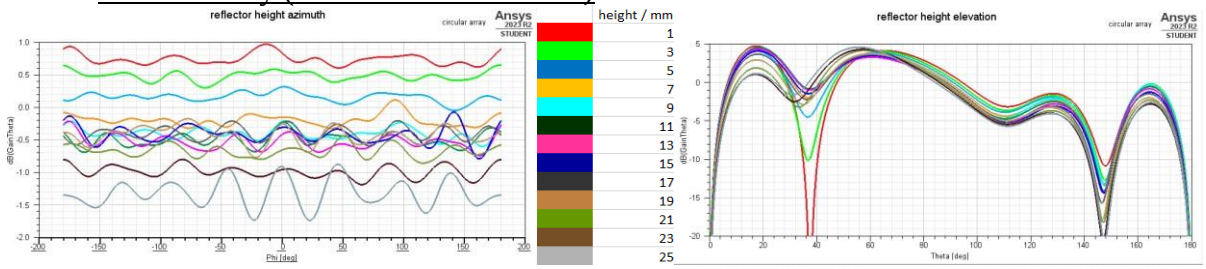


**Fig. 2**: Gain for array of reflector height 1-25mm with all ports excited

| HEIGHT / mm | 1 | 3 | 5 | 7 | 9 | 11 | 13 | 15 | 17 | 19 | 21 | 23 | 25 |
|---|---|---|---|---|---|---|---|---|---|---|---|---|---|
| MIN / dB | 0.61 | 0.30 | -0.05 | -0.32 | -0.60 | -0.69 | -0.74 | -0.79 | -0.59 | -0.77 | -0.85 | -1.18 | -1.73 |
| MAX / dB | 0.97 | 0.65 | 0.32 | 0.11 | -0.21 | -0.23 | -0.21 | -0.08 | -0.21 | -0.17 | -0.44 | -0.80 | -0.87 |
| DEVIATION / dB | 0.36 | 0.34 | 0.36 | 0.43 | 0.39 | 0.46 | 0.53 | 0.71 | 0.39 | 0.59 | 0.42 | 0.39 | 0.86 |
| AVG / dB | 0.74 | 0.48 | 0.16 | -0.20 | -0.40 | -0.50 | -0.53 | -0.42 | -0.40 | -0.42 | -0.67 | -0.98 | -1.32 |

**Table 1**: Azimuthal gain of array vs height of reflector

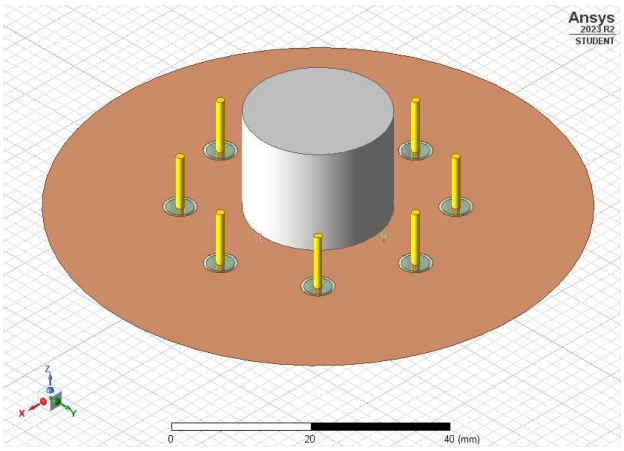


**Fig. 3:** Circular array setup in HFSS

At θ = 90° (azimuth), the average gain of the array decreases as reflector height increases, while the ripple size (deviation from min to max gain) varies arbitrarily. As seen from the elevation plot at ϕ = -13.5°, there is a null point at θ = 38° for reflector height = 1mm, which allows more of its gain to be directed further on the azimuth plane. Hence, in terms of omnidirectional radiation on the azimuth plane, a lower reflector height is optimal.

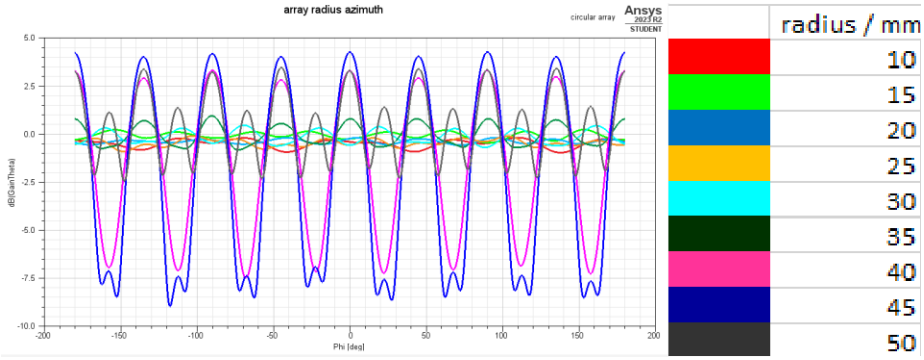


**Fig. 4:** Azimuthal gain for array of radius 10-50mm with all ports excited

| RADIUS / mm | 10 | 15 | 20 | 25 | 30 | 35 | 40 | 45 | 50 |
|---|---|---|---|---|---|---|---|---|---|
| MIN / dB | -1.02 | -0.91 | -0.60 | -1.37 | -4.03 | -2.55 | -7.79 | -11.54 | -5.19 |
| MAX / dB | -0.38 | -0.38 | -0.21 | -0.89 | -2.73 | 1.05 | 3.65 | 4.02 | 2.41 |
| DEVIATION / dB | 0.63 | 0.53 | 0.39 | 0.48 | 1.30 | 3.59 | 11.44 | 15.56 | 7.60 |
| AVG / dB | -0.61 | -0.64 | -0.40 | -1.11 | -3.33 | -0.70 | -1.15 | -3.37 | -0.69 |

**Table 2**: Azimuthal gain of array vs radius of array

As the array radius increases, ripples in the radiation pattern form and increase in size. From array radius = 10-25mm, the gain of the array remains flat with little to no ripples. At array radius = 50mm, there are twice as many ripples present as more waves converge between elements. As a radiation pattern with few ripples provides better coverage, a smaller array radius is desired for omnidirectional radiation. From Table 2, a 20mm array radius provides the highest average gain and lowest ripple magnitude.

3. Circular array (Directional mode)

To achieve directional radiation, only a few elements would have to be excited in the desired radiation direction.

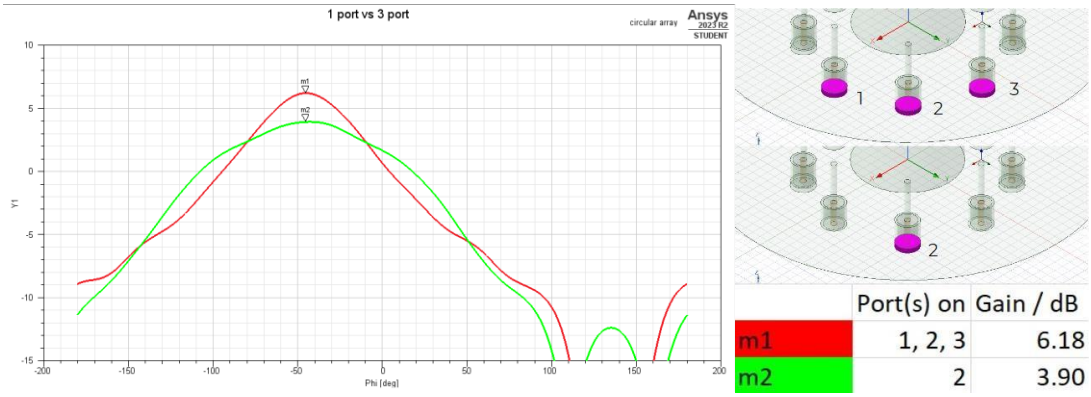


**Fig. 5**: Azimuthal gain of array when exciting 1 element (green) vs 3 adjacent elements (red)

Exciting 3 adjacent ports provides a higher gain of 6.18dB in the desired direction ($\phi$ = -45°) as compared to exciting 1 port, which gives 3.90dB, although the gain of the single port excitation is comparatively higher in the directions surrounding the desired one. Hence, to direct gain at intervals of 45°, 3 adjacent ports should be excited.

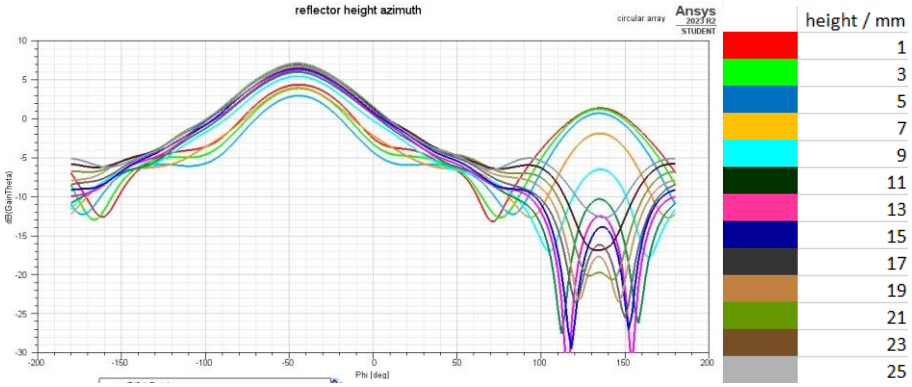


**Fig. 6**: Azimuthal gain for array of reflector height 1-25mm with 3 ports excited

As the reflector height increases, the gain in the desired direction increases. Hence in the directional mode, a higher reflector height is optimal. However, as seen from Fig. 2, a higher reflector height performs worse in the omnidirectional mode (all ports excited). Hence, a compromise between the two modes is needed.

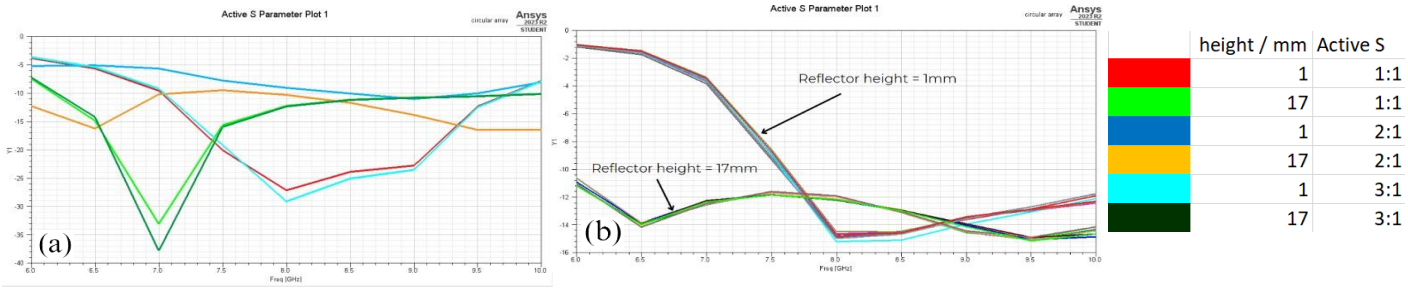


**Fig. 7**: Active S Parameter for reflector height of 1mm and 17mm for (a) 3 excited ports (b) all excited ports

Although the gain of the array is viable at reflector height = 1mm, (a) the S21 of port 2 suffers greatly, and (b) a better than -10dB return loss is displayed from 7.6GHz. Hence, a low reflector height would affect the S11 performance and is not viable.

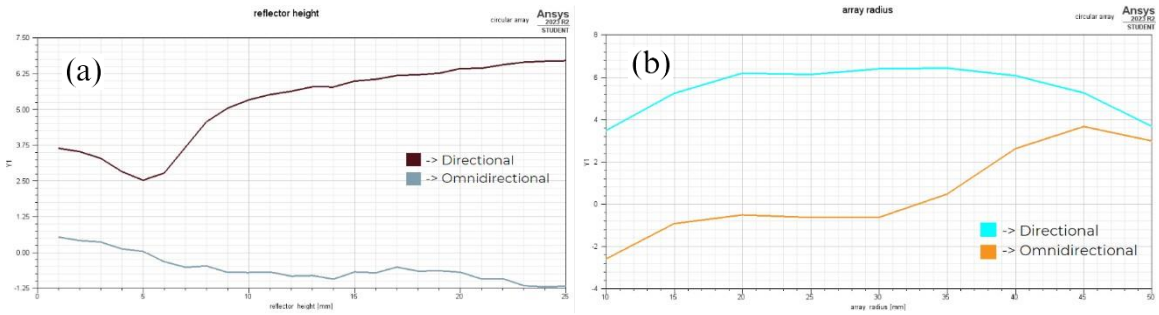


**Fig. 8**: Omnidirectional and directional gain for (a) reflector height of 1-25mm (b) array radius of 10-50mm

From this, we decided that a higher reflector height would provide the best trade-off between omnidirectional gain and directional gain. A reflector height of 17mm would have 1dB less average omnidirectional gain than a 1mm reflector height, but would provide 2.2dB more of directional gain. An array radius of 20mm provides the highest directional and omnidirectional gain from array radii of 10-25mm (where ripples are minimised).

4. <u>Phase excitation</u>

Due to the circular nature of the array, during 3 port radiation, the elements are not in line with one another. This physical displacement causes their radiation to not be in phase. To mitigate this effect, we investigated phase shifts to maximise directional gain in the 3-port excitation mode.

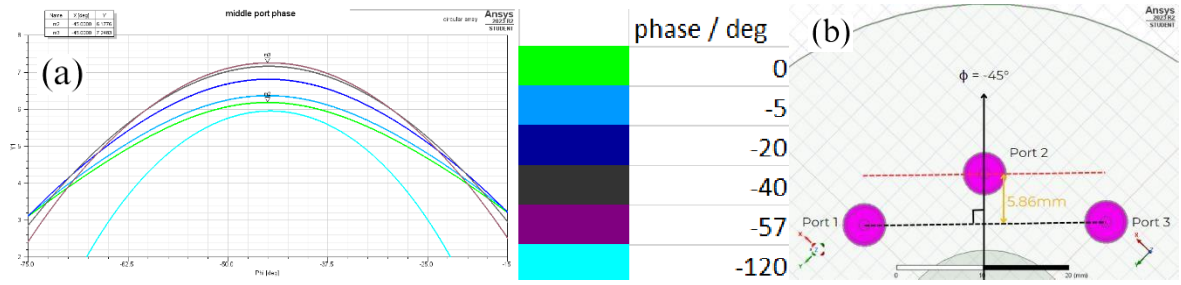


**Fig. 9**: (a) Directional gain of array when varying middle port phase (b) Phase change diagram

As the phase of port 2 decreases from 0° to -57°, directional gain increases from 6.2dB to 7.2dB. This phase can be derived from the physical displacement between the central port and the 2 side ports as measured in HFSS, where a 360° phase delay would compensate for a 3.75cm (1 wavelength) offset at an operating frequency of 8GHz.

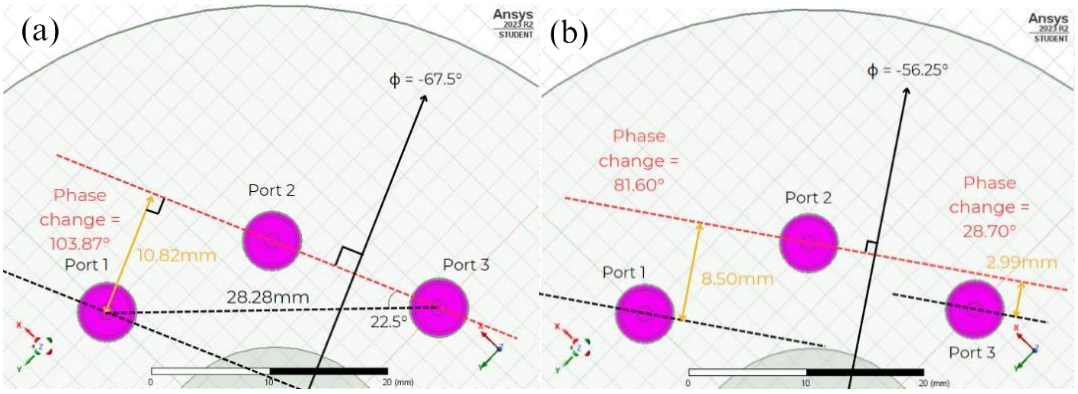


**Fig. 10**: Phase shifting for ϕ = (a) -56.25° (b) -67.5°

The distances in the diagram were measured using HFSS, to calculate the respective phase changes needed for each element $(360° = 3.75cm,\ 1° = 0.010417cm)$. However, the distances can also be calculated mathematically, as shown below. The general formula of deriving phase change, in degrees, for an element at any angle would thus be: $\frac{d}{\frac{\lambda}{360}}$, where d is the distance between the element and the perpendicular wavefront of the reference port and λ is wavelength given by $\lambda = \frac{3.0\times10^8}{f}$(f is centre frequency).

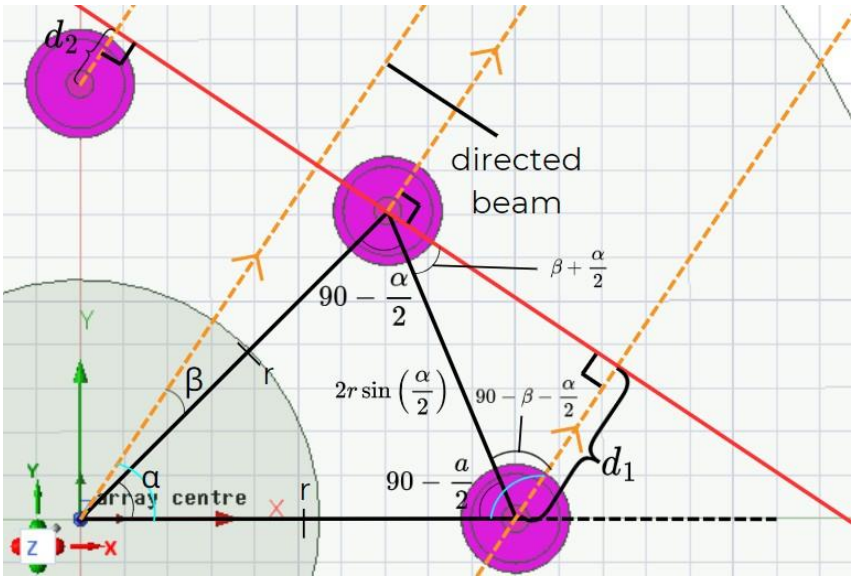


**Fig. 11:** Derivation of general formula

The distance d can be calculated by:

$$d = 2r\sin\left(\frac{\alpha}{2}\right)\cos\left(90 - \beta - \frac{\alpha}{2}\right) = 2r\sin\left(\frac{\alpha}{2}\right)\sin\left(\beta + \frac{\alpha}{2}\right),$$

where r is the array radius measured from centre of array to any element, β is the angle between port 2 and the directed gain, and α is the angle between adjacent elements given by $\frac{360°}{no.\ of\ elements}$. When using the antenna in its 3-port directional mode, two elements would usually require a

phase change, with the middle port taken as reference, except when $\beta = 0°$ or $\pm 22.5°$ as shown in Fig. 8(b) and 9(b), where the wavefront of the directed beam aligns parallel with two ports, resulting in only one port needing a phase change.

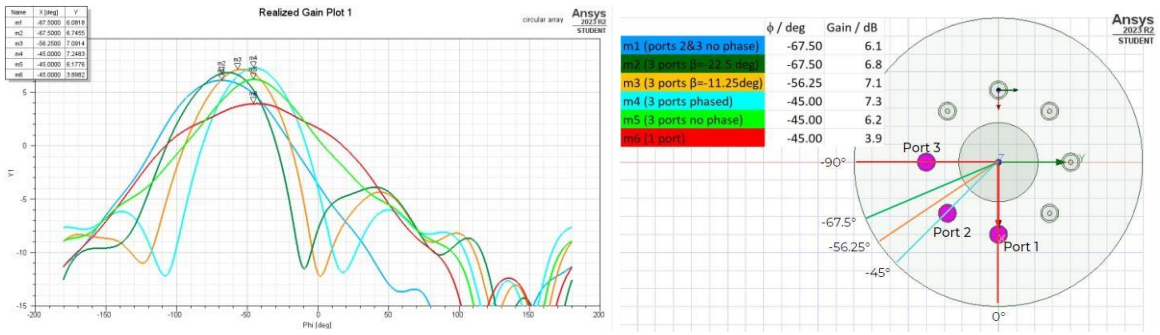


**Fig. 12:** Beam steering with phased array

By manipulating the phases of each element, we found that we can steer the main beam in any desired direction. Fig. 12 shows that beam steering with phased elements consistently provides more gain than with no phase. Hence, phase shifts electronically "align" the elements, maximising constructive interference. In the directional mode, the array would thus have a gain from 6.8 to 7.3dB.

5. Fabrication of array

**Fig. 13:** Photos of fabricated array (left) Side view (centre) Top view (right) Bottom view

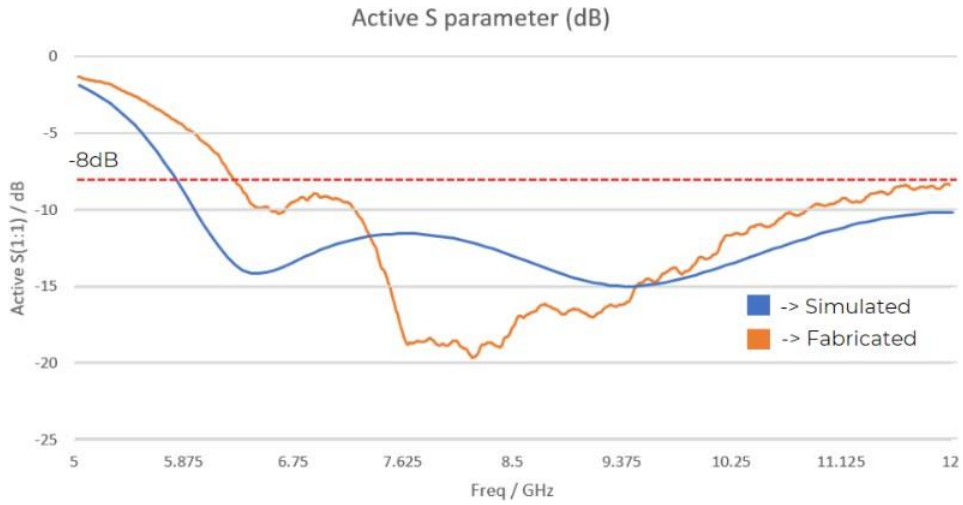


**Fig. 14:** Measured active S11 of fabricated array and simulated active S11 with HFSS

The base structure and reflector of the array were 3D printed, and metallised using copper and aluminum tape respectively. 8 SMA connectors were used as monopoles, after cutting the centre pin to 9mm of height. The array was then tested using a 2-port VNA system, measuring the S11, S12, S21 and S22 parameters. The feeding coaxial cable has a 50Ω characteristic impedance. The measured active S11 of the fabricated antenna follows a similar trend to the simulated result, only performing slightly poorer. The simulated active S11 is entirely below -10dB from 6-10GHz, while the measured active S11 performs better at the antenna's intended centre frequency with a lower return loss of -18.5dB compared to the simulated value of -11.9dB. Taking roughly -8dB instead as the viable return loss, the measured impedance bandwidth is 6-12GHz. The small discrepancies can be attributed to potential inconsistencies due to variation in antenna position and height at which it is held during testing. Additionally, there were slight imperfections in the fabrication of the antenna due to human error, like the crumpling of the metal tape.

## DISCUSSION

Especially when the receiver is of a far distance away from the antenna, the difference in elevation between the two becomes negligible. Hence, our area of focus would be on the azimuthal (horizontal) radiation of the array, where $\theta = 0°$.

| Simulated realised average omnidirectional gain / dB | Simulated realised directional gain / dB | Simulated 10dB return loss bandwidth (Omnidirectional) | Simulated 10dB return loss bandwidth (Directional) | Measured 8dB return loss bandwidth (Omnidirectional) |
|---|---|---|---|---|
| -0.68 | 6.8-7.3 ($\beta = 0°$ to $\pm 22.5°$) | 6-10GHz | 6.2-10GHz | 6-12GHz |

**Table 3:** Simulated and measured performance of circular array (Array radius 20mm, reflector height 17mm)

It is worth noting that the gain of our fabricated array was not measured due to logistical constraints. More complex element shapes can also be arrayed to study their performance. These can be investigated in further work. Overall, our array has fulfilled our performance criteria and can be used as a versatile antenna, covering both directional and omnidirectional radiation, providing an adaptable alternative to the conventional monopole.

## REFERENCES

[1] N. Tohme, J. -M. Paillot, D. Cordeau, S. Cauet, Y. Mahe and P. Ribardiere, "A 2.4 GHz 1-dimensional array antenna driven by vector modulators," 2008 IEEE MTT-S International Microwave Symposium Digest, Atlanta, GA, USA, 2008, pp. 803-806.

[2] N. H. Noordin, V. Zuniga, A. O. El-Rayis, N. Haridas, A. T. Erdogan and T. Arslan, "Uniform circular arrays for phased array antenna," 2011 Loughborough Antennas & Propagation Conference, Loughborough, UK, 2011, pp. 1-4.

## APPENDIX

In this section, additional information is provided. Supplementing graphs of lesser importance or additional photos of fabrication and testing are placed here, followed by a page number that the reader should reference for context on the graphs and how they factor into design.

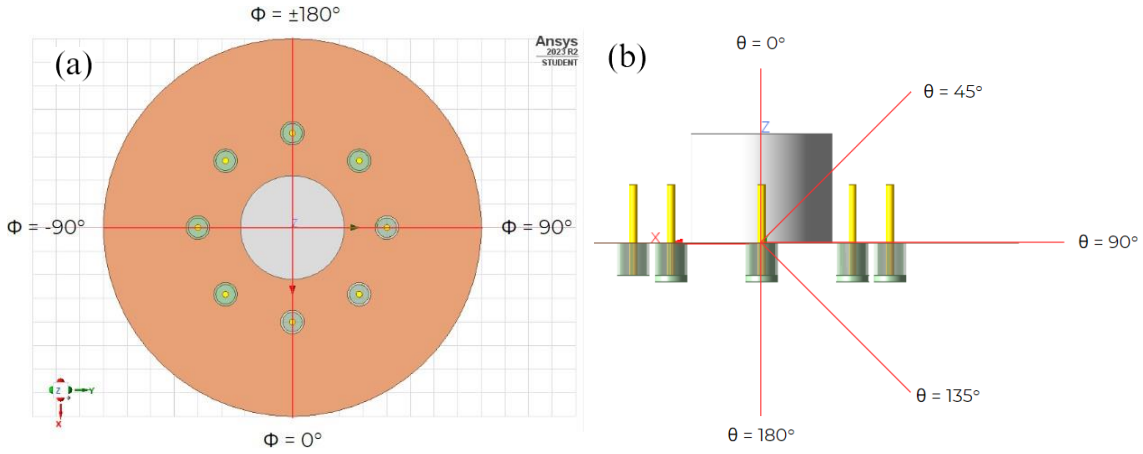


**Fig. 1 (page 2-7):** Setup and spherical angles (a) azimuth (b) elevation

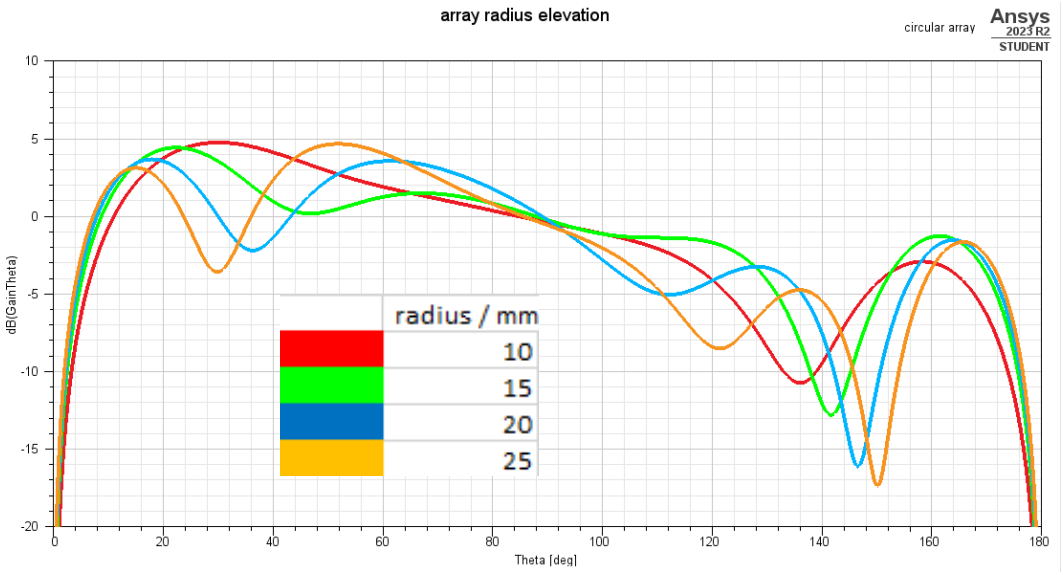


**Fig. 2 (page 3):** Elevation gain for array of radius 10-25mm with all ports excited

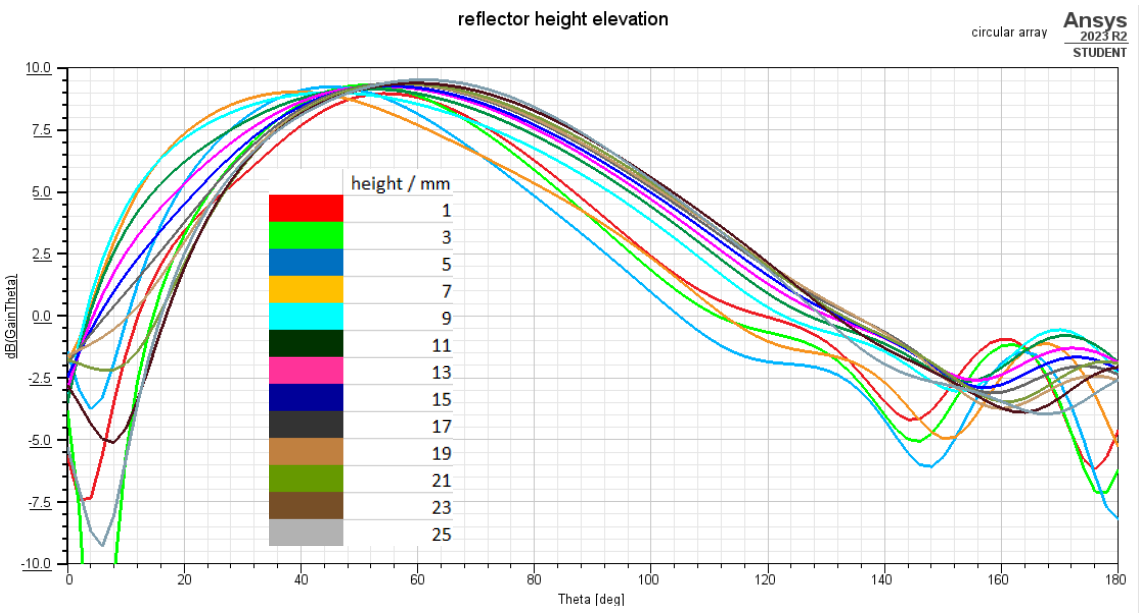


**Fig. 3 (page 4):** Elevation gain for array of reflector height 1-25mm with 3 ports excited

**Fig. 4 (page 7-8):** Rohde and Schwarz ZNB20 Vector Network Analyzer used to measure S11 of fabricated antenna